THE ASTROPHYSICAL JOURNAL, 391:L75–L79, 1992 June 1

AN X-RAY IMAGE OF THE SEYFERT GALAXY NGC 1068

A. S. WILSON[1]
Astronomy Department, University of Maryland, College Park, MD 20742; and Space Telescope Science Institute, 3700 San Martin Drive, Baltimore, MD 21218

M. ELVIS[1]
Harvard Smithsonian Center for Astrophysics, 60 Garden Street, Cambridge, MA 02138

A. LAWRENCE[1]
Physics Department, Queen Mary and Westfield College, University of London, Mile End Road, London E1 4N2, England, UK

AND

J. BLAND-HAWTHORN[1]
Department of Space Physics and Astronomy, Rice University, Houston, TX 77251-1892
Received 1992 January 21; accepted 1992 March 18

ABSTRACT

We present and discuss an image of NGC 1068 with resolution 4″–5″ obtained with the High Resolution Imager on the *ROSAT* X-ray Observatory in the energy band 0.1–2.4 keV. The map shows a compact nuclear source, circumnuclear extended (diameter $\simeq 1.5$ kpc) emission, and emission on a scale (diameter ≈ 13 kpc) similar to the starburst disk. The circumnuclear emission extends preferentially toward the NE, the same direction as found in several other wavebands. We favor thermal emission from a hot (10^{6-7} K), outflowing wind as the source of the nuclear and circumnuclear emission. This hot gas has a similar pressure to that of the optical line-emitting filaments in the lower density narrow-line region, and may be responsible for their confinement. The large-scale X-rays are probably dominated by emission from the starburst disk, although a contribution from an extension of the nucleus-driven wind to large radii is possible. The X-ray spectrum of the starburst disk is found to be harder than that of the nucleus. Emission from the starburst, rather than the electron-scattered Seyfert nucleus, may be responsible for much of the hard spectrum emission from NGC 1068 in the 2–10 keV band. Recent modeling of the electron-scattering cone in this galaxy has required the optical depth to photoelectric absorption near 1 keV to be ≤ 1, but this constraint is unnecessary if most of the X-ray emission comes from spatial scales comparable to the starburst and the narrow-line region.

Subject headings: galaxies: individual (NGC 1068) — galaxies: interstellar matter — galaxies: jets — galaxies: nuclei — galaxies: Seyfert — X-rays: galaxies

1. INTRODUCTION

Studies of spatially extended, soft X-ray emission in active galaxies may yield valuable information about the interaction between the active galactic nucleus (AGN) and its surroundings. Thermal bremsstrahlung emission from hot gas should be ubiquitous, for such gas may be generated in shock waves produced through collisions between high-velocity clouds in the narrow-line region (NLR), or through entrainment of interstellar clouds in a radio jet, a radio lobe, or an outflowing wind. Extended X-ray emission associated with AGN can also result from synchrotron radiation or inverse Compton scattering. X-rays generated by the compact, nuclear X-ray source may be scattered by electrons in the interstellar medium and be seen as an X-ray "halo."

The nearby (15 Mpc, for $H_0 = 75$ km s^{-1} Mpc^{-1}), luminous [$(2–3) \times 10^{11}$ $L_\odot$] Seyfert galaxy NGC 1068 is an obvious candidate for extended X-ray emission, for it contains high-velocity (up to $\simeq 1000$ km s^{-1}) gas clouds in the inner $\simeq 15''$–$20''$ (1.1–1.5 kpc; e.g., Cecil, Bland, & Tully 1990) and a "linear" radio source, with extent 13″ (950 pc), which is apparently fueled by collimated ejection from the active nucleus (Wilson & Ulvestad 1982). Further, X-rays should be produced by supernova remnants and X-ray binaries associated with the luminous, 30″ (2.2 kpc) scale, disk "starburst" (e.g., Bruhweiler, Truong, & Altner 1991; Telesco et al. 1984). Although the spectrum of the *integrated* X-ray emission of NGC 1068 has been measured (Monier & Halpern 1987; Elvis & Lawrence 1988), no studies of its spatial distribution have been published.

A quite different motivation for searching for extended, soft X-ray emission from NGC 1068 is related to the properties of the nuclear, electron scattering zone. Antonucci & Miller (1985) found that the spectrum of NGC 1068 (classically a Seyfert galaxy of type 2) in linearly polarized light resembles the spectrum of a Seyfert 1 galaxy. They proposed that the galaxy contains a Seyfert 1 nucleus blocked from direct view by a thick torus, but rendered visible through scattering by a cloud of electrons along the axis of the torus. Miller, Goodrich, & Mathews (1991) have inferred an electron temperature of less than 3×10^5 K for the scattering cloud from limits to broadening of Hβ by the scattering. This low temperature must be reconciled with the high level of ionization implied by the absence of photoelectric absorption in the X-ray spectrum (Elvis & Lawrence 1988) and by the observed energy of the Fe Kα line (Koyama et al. 1989). As described in detail by Miller, Goodrich, & Mathews (1991), models satisfying these contrasting constraints are possible, but the range allowed for the physical parameters describing the scattering zone is uncomfortably small. The constraints would be eased if some of the X-ray emission originates from larger scales than the scattering zone, and therefore does not have to pass through it.

In order to image NGC 1068 in soft X-rays, we have observed it with the High Resolution Imager (HRI) on the *ROSAT* X-Ray Observatory. The galaxy was observed

[1] Guest Observer, *ROSAT* Observatory.

between 1991 July 24 and 26, for a total integration time ("live time") of 19,947 s. The image shows obvious extended structure, which is reported here.

2. RESULTS

The spatial resolution of the unsmoothed image can be estimated from a compact X-ray source located 347″ S and 54″ E of the nucleus of NGC 1068. This source contains 218 counts and is probably associated with a ≈ 15 mag stellar object. An azimuthally averaged, radial profile reveals a FWHM of 4″–5″, and a 50% power radius of $\simeq 3\farcs7$, consistent with other HRI observations processed using the current aspect solution (see also Fig. 3).

Contour maps of the X-ray brightness distribution of NGC 1068 are shown in Figure 1. The data have been smoothed with circular Gaussians of FWHM 1″, 2″.5, and 5″ in Figures 1*a*, 1*b*, and 1*c*, respectively. While residual errors in the aspect solution render fine scale (a few arcseconds) details uncertain, Figure 1*a* reveals a compact source within 3″ of the optical nucleus (Clements 1981), plus emission extending asymmetrically to the N and NE. The highest resolution map suggests the presence of localized "ridges" at 6″–12″ from the nucleus toward the NE (P.A. $\simeq$ 10°–35°). At larger distances (15″–60″) from the nucleus, fainter X-ray emission is found aligned along P.A. 35°–45° to both NE and SW of the nucleus (Fig. 1*c*). The *ROSAT* HRI has some energy resolution, and the pulse height distributions for the nuclear emission, the circumnuclear emission, and the very extended emission are all *inconsistent* with that found for signals dominated by uv contamination (as appears to be the case for an HRI observation of Vega; [M. Zombeck, private communication]).

Extensions from the nucleus of NGC 1068 toward the N and NE are seen on the arcseconds or subarcseconds scale in several other wavebands, including radio continuum (Ulvestad, Neff, & Wilson 1987), mid-infrared (Tresch-Fienberg et al. 1987), optical emission line (Pogge 1989; Evans et al. 1991), and optical continuum (Balick & Heckman 1985; Lynds et al. 1991). The axis (P.A. 35°–45°) of the larger scale X-ray emission (Fig. 1*c*) may be compared with the major axis (p.a. 50°–55°) of the ovally distorted disk on the 40″ (diameter) scale (Baldwin, Wilson, & Whittle 1987), and the direction (p.a. 48°) of the 36″ length stellar bar seen at 2 μm (Scoville et al. 1988). Figure 2 (Plate L6) shows the low-resolution image superimposed on a blue band photograph. It can be seen that the outer X-ray contours follow the edge of the brightest part of the visible disk quite well, and there are suggestions of associations between details of the emission in the two wavebands. The overall similarity of this faint, outer X-ray emission to the optical image suggests that it is associated with the "starburst" disk, and presumably represents emission from supernova remnants, X-ray binaries, and possibly a starburst-driven wind. We prefer this interpretation to the alternative, which would explain this outer emission in terms of a large-scale wind driven by the Seyfert nucleus (see § 3.1).

An azimuthally averaged radial profile is shown in Figure 3. The data suggest faint emission to a radius of $\simeq 1\farcm5$, although the reality of the outermost emisson must be considered uncertain until improved calibrations of the HRI are available. In order to estimate the fraction of the emission which is extended, a point spread function (Fig. 3) was first obtained from three calibration sources. This point spread function was then scaled to the peak flux at the nucleus of NGC 1068 and subtracted from it. The result is that 45% $\pm$ 5% of the total detected HRI flux is spatially extended.

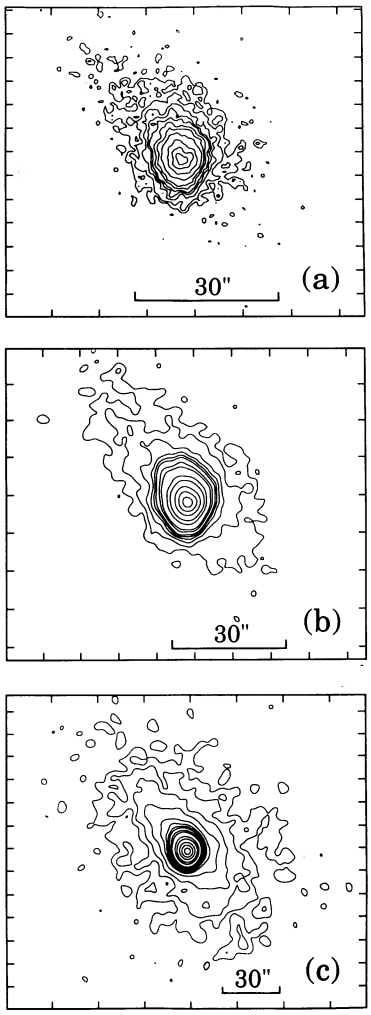

FIG. 1.—Contour maps of the distribution of X-ray emission in NGC 1068. North is up, and east is left. In order to show the X-ray emission on different spatial scales, the data have been smoothed with different Gaussian functions in the three panels. The peak brightnesses listed are for the *ROSAT* HRI band *before* photoelectric absorption, assuming a power-law spectrum of index $\alpha_E = 2.0$ and a hydrogen column $N_h = 3 \times 10^{20}$ cm^{-2}. (*a*) Smoothing function is 1″ (FWHM). Contours are plotted at 1.25, 2.5, 5, 7.5, 10, 15, 20, 30, 50, 70, and 90% of the peak brightness of 37.9 counts pixel^{-1} (1 pixel = 0″.5 × 0″.5) or 7.7×10^{-13} ergs cm^{-2} s^{-1} (arcsec)$^{-2}$. (*b*) Smoothing function is 2″.5 (FWHM). Contours are plotted at 0.5, 1, 2, 3, 4, 5, 7.5, 10, 20, 30, 50, 70, and 90% of the peak brightness of 32.3 counts pixel^{-1} or 6.6×10^{-13} ergs cm^{-2} s^{-1} arcsec^{-2}. (*c*) Smoothing function is 5″ (FWHM). Contours are plotted at 0.125, 0.25, 0.5, 1, 2, 3, 4, 5, 7.5, 10, 20, 30, 50, 70, and 90% of the peak brightness of 23.2 counts pixel^{-1} or 4.7×10^{-13} ergs cm^{-2} s^{-1} arcsec^{-2}.

Within a radius of 100″ from the nucleus, the total count rate is 0.57 counts s^{-1} (after background subtraction). If we adopt the spectral parameters obtained by Monier & Halpern (1987) from *Einstein* IPC observations, namely, an intrinsic (unabsorbed) flux of 5.8×10^{-11} ergs cm^{-2} s^{-1} in the *ROSAT* band (0.1–2.4 keV), a power-law spectrum of energy index $\alpha_E = 2.0$ [so $F_E \simeq 2.5 \times 10^{-29}(E/keV)^{-2}$ ergs cm^{-2} s^{-1} Hz^{-1}], and a hydrogen column $N_h = (3\text{–}5) \times 10^{20}$ cm^{-2}, a total *ROSAT* HRI count rate of 0.56–0.36 counts s^{-1} is predicted. The good agreement between the first of these predicted count rates and that observed with *ROSAT* confirms that the hydrogen column density is close to the Galactic value of $N_h = 3.0 \times 10^{20}$ cm^{-2} (Elvis & Lawrence 1988).

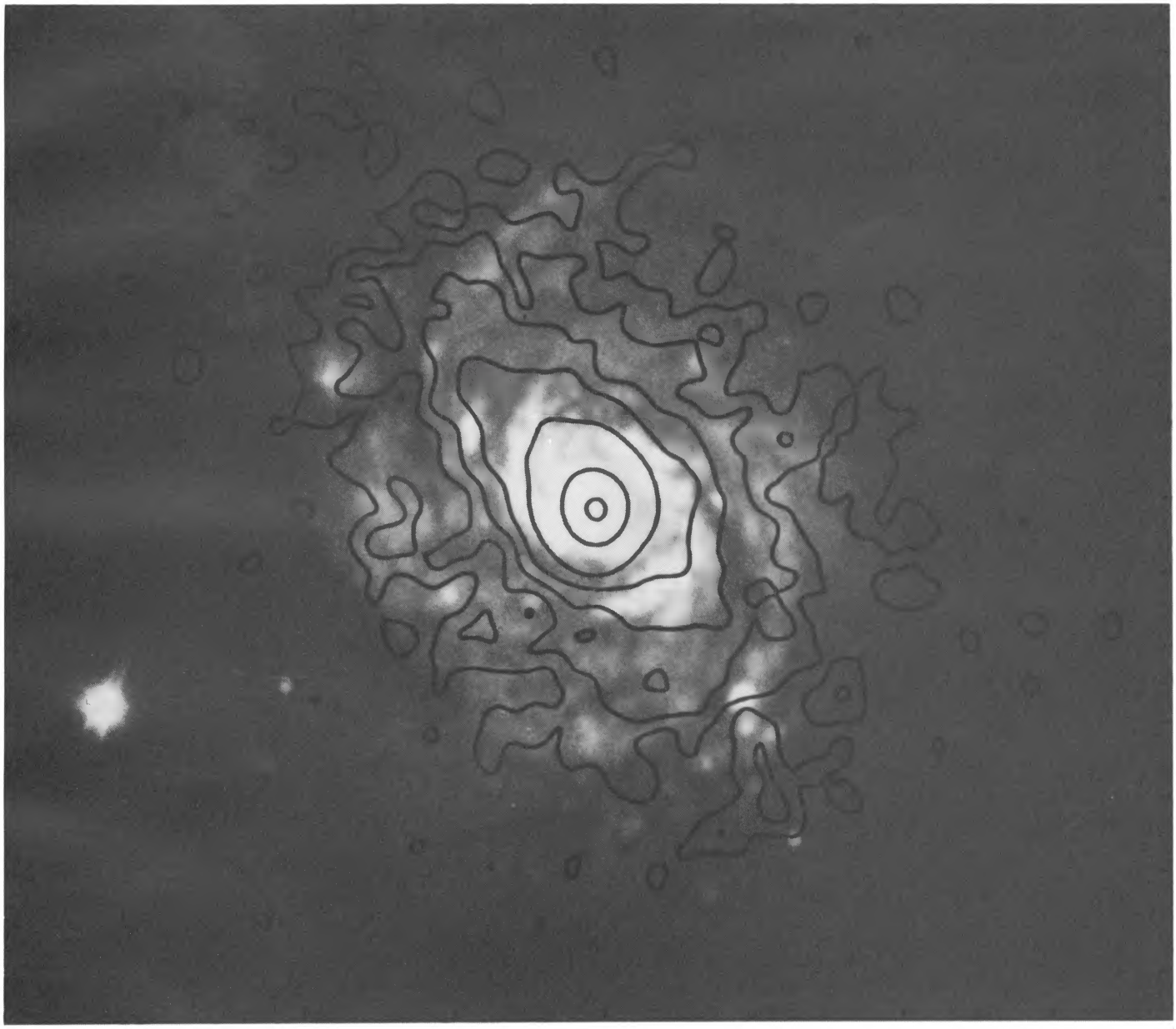

FIG. 2.—Contour map of the X-ray data (smoothed with a 5″ FWHM Gaussian function) superposed on a blue (IIaO emulsion) print from the Hubble atlas (Sandage 1961). North is up and east is to the left. Contours are plotted at 0.125, 0.25, 0.5, 1, 3, 30, and 90% of the peak brightness. The tick marks along the horizontal and vertical axes are separated by 25″ and 12.″5, respectively (the field size is 3.′23 E–W × 2.′82 N–S).

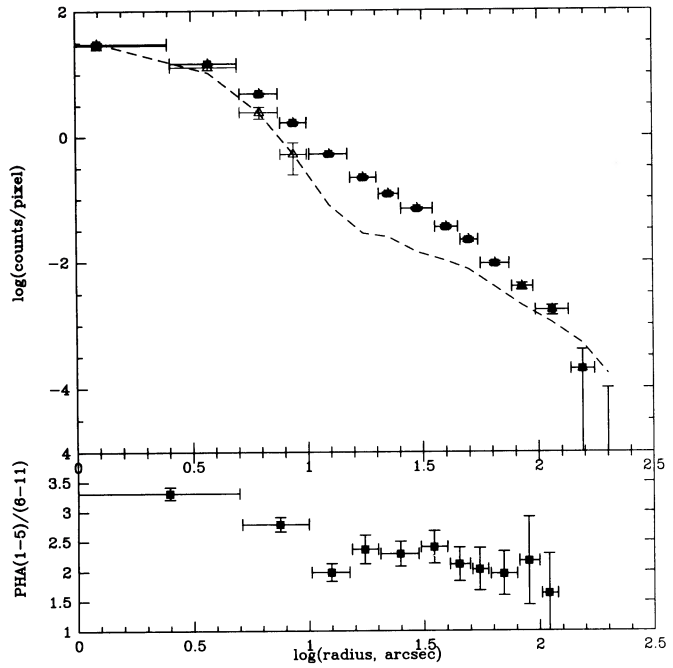

FIG. 3.—The top panel shows the log of the azimuthally averaged number of counts per pixel for NGC 1068 (*filled symbols*), the star 6′ to the S of NGC 1068 (*open triangles*), and the point spread function derived from the average of the calibration sources LMC X-1, HZ43 and ARLac (*dashed line*) plotted against log radius (distance from peak flux). The lower panel is a plot of the "softness ratio" (counts in PHA channels 1–5 divided by counts in PHA channels 6–11) for NGC 1068 vs. log radius. This ratio is seen to decrease (i.e., the spectrum hardens) with increasing radius.

It is clear that the spectrum of the nuclear source is much softer than that of the very extended emission more than 10″ from the nucleus (Fig. 3). At this early stage in the *ROSAT* pointed phase, no good calibration of the HRI energy response has been made, so a full investigation of the spectral characteristics of the different components in NGC 1068 must be deferred to a later paper. Nevertheless, the steep spectrum emission seen with the *Einstein* IPC (Monier & Halpern 1987) must originate in the nucleus and possibly also the circumnuclear region. In the following section, we argue that the hard component (with $F_E \propto E^{-0.5}$) detected from NGC 1068 in the 2–10 keV band (Elvis & Lawrence 1988; Koyama et al. 1989) may be dominated by emission from the extended starburst, rather than the Seyfert nucleus as has usually been assumed.

3. DISCUSSION

Our observations show that the soft X-ray emission of NGC 1068 comprises an unresolved source associated with the Seyfert nucleus, emission extending from the nucleus on the several arcsecond scale, and large-scale emission reaching $\simeq 1'.5$ (6.6 kpc) from the nucleus. Broad optical emission lines are detected out to the inner edge of the molecular ring, some 10″ (730 pc) from the nucleus (Baldwin, Wilson, & Whittle 1987), and delineate the extent of the kinematic influence of the nuclear activity. The brightest X-ray emission is also contained within $\simeq 10''$ of the Seyfert nucleus. The large-scale emission correlates quite well with the starburst disk (Fig. 2 [Pl. L6]), although some of this X-ray emission could be fueled by the nucleus (e.g., as a large-scale wind), given its rough alignment with the nuclear elongation. Of the total count rate, some 55% (3.2×10^{-11} ergs cm^{-2} s^{-1} before photoelectric absorption and assuming a power-law spectrum with $\alpha_E = 2.0$) then represents *unresolved* nuclear emission, $\simeq 23\%$ (1.3×10^{-11} ergs cm^{-2} s^{-1}) is *extended* nuclear emission, and the remaining 22% (1.3×10^{-11} ergs cm^{-2} s^{-1} for the above power-law spectrum, or 5.7×10^{-12} ergs cm^{-2} s^{-1} for thermal bremsstrahlung emission with $kT = 5$ keV) originates in the starburst disk. The corresponding X-ray luminosities are 8×10^{41}, 3×10^{41}, and $(3–1.4) \times 10^{41}$ ergs s^{-1}, respectively. Although the quantitative separation between nucleus and starburst disk is somewhat arbitrary, it seems clear that both contribute to the X-ray emission, so in the following discussion we consider the likely emission processes separately.

3.1. *The X-Ray Emission of the Nucleus*

The unresolved and extended nuclear X-rays could result from synchrotron radiation, inverse Compton scattering, thermal emission processes or electron scattering of an unresolved nuclear source. We discuss each of these possibilities in turn.

3.1.1. *Synchrotron Radiation*

Synchrotron radiation in the *ROSAT* band would require relativistic electrons with $\gamma \simeq 10^7$ given the equipartition magnetic fields of 10^{-4}–10^{-3} G in the radio core and lobes (e.g., Wilson & Ulvestad 1987). The synchrotron half-lives would be only $\simeq 1$–10 yr. The half-lives of these electrons to inverse Compton scattering can be even shorter in regions close to the nucleus where the energy density in mid-infrared photons is larger than that of the magnetic field. For these reasons, we consider a synchrotron model implausible.

3.1.2. *Inverse Compton Radiation*

The observed photon energy density close to the nucleus of NGC 1068 is dominated by radiation with wavelengths near 20 μm (Telesco et al. 1984). Upward scattering of these photons to $\simeq 1$ keV requires relativistic electrons with $\gamma \simeq 100$. Such electrons would radiate synchrotron radiation at frequencies of MHz to tens of MHz. The total radio power emitted in the 1–100 MHz band is only $\simeq 1 \times 10^{39}$ ergs s^{-1}, a factor of 1000 below the observed nuclear emission in the *ROSAT* band. Thus, a viable inverse Compton model would require these electrons to lose energy primarily to the radiation field. If the relativistic electrons are confined to the observed radio features, the magnetic field needs to be well below equipartition. Alternatively, a large population of relativistic electrons outside the radio features, where the field could be very weak, would be required.

3.1.3. *Thermal Emission*

A more promising model for the extended, nuclear X-rays is thermal emission from hot gas in a nucleus-driven wind. Assuming the gas is in collisional equilibrium at a temperature of 10^6–10^7 K and that the X-rays extend to 10″ (730 pc) from the nucleus, a density (assumed uniform) of 2.2–0.9 cm^{-3} is required to account for the X-ray luminosity (Raymond & Smith 1977). The mass of hot gas is $(9–4) \times 10^7\ M_\odot$ in this model, but would be less if the gas is clumped. The pressure of this hot component would be $\simeq (3–12) \times 10^{-10}$ ergs cm^{-3}. This value is comparable to that required to confine the optical line-emitting filaments in the lower density narrow-line region (Shields & Oke 1975), for which the density, temperature, and pressure are $\simeq 800$ cm^{-3}, $\simeq 10^4$ K and $(7–11) \times 10^{-10}$ ergs cm^{-3}, respectively. This result supports models in which the cool, optical line-emitting filaments condense out of, or are

entrained by, a hot, outflowing wind (e.g., Krolik & Vrtilek 1984).

3.1.4. *Electron-scattered Nuclear Radiation*

Elvis et al. (1990) have argued against electron-scattered nuclear radiation as the source of the *spatially extended*, soft X-ray emission detected from several Seyfert galaxies. They noted that the extended gas must be sufficiently highly ionized that it does not absorb the X-rays. If this is achieved thermally, a temperature above $\simeq 3 \times 10^6$ K is needed, and direct bremsstrahlung then dominates over scattered radiation. If it is achieved radiatively, the ionization parameter of the gas at distances of 0.3–1 kpc from the nucleus must be so high that the luminosity of the central source becomes much larger than is observed. Application of this argument to the circumnuclear X-ray emission of NGC 1068 gives a required central luminosity of $\geq 2 \times 10^{46}$ ergs s^{-1}. This number is more than an order of magnitude above the observed bolometric luminosity of the nucleus of NGC 1068, rendering implausible an electron scattering model for the *extended* nuclear emission.

3.2. *The X-Ray Emission of the Starburst*

Fabbiano & Trinchieri (1985) have found an approximately linear correlation between X-ray and blue luminosities for the disks of spiral galaxies, and they concluded that the X-ray emission of spirals is largely connected with the Population I component. It is then of interest to see whether the starburst disk of NGC 1068 conforms with this relation. Adopting $B_T^0 = 9.17$ (de Vaucouleurs, de Vaucouleurs, & Corwin 1976) and subtracting off the nuclear contribution, we find $f_B = 8.2 \times 10^{-24}$ ergs cm^{-2} s^{-1} Hz^{-1} for the disk alone. Assuming the disk emission is thermal with a temperature $kT = 5$ keV, $f_{2\,\mathrm{keV}} = 7.1 \times 10^{-30}$ ergs cm^{-2} s^{-1} Hz^{-1}, so $f_{2\,\mathrm{keV}}/f_B = 8.7 \times 10^{-7}$. This ratio is larger than is typical of normal spirals, for which the distribution of $f_{2\,\mathrm{keV}}/f_B$ peaks near $\simeq 1.6 \times 10^{-7}$ (Fabbiano & Trinchieri 1985), but is two to three orders of magnitude lower than that for type 1 Seyfert galaxies. The ratio for the disk of NGC 1068 is, however, similar to those found for peculiar galaxies experiencing bursts of star formation (Fabbiano, Feigelson, & Zamorani 1982). A further comparison may be made with the results of Griffiths & Padovani (1990), who showed that the average of the X-ray to far-infrared luminosity ratio $\log L(0.5\text{–}3.0\ \mathrm{keV})/L(60\ \mu\mathrm{m}) = -3.32 \pm 0.10$ for *IRAS* galaxies and $= -3.27 \pm 0.11$ for starburst/interacting galaxies. For the disk of NGC 1068, this ratio is -3.27. These similarities with galaxies undergoing active star formation are consistent with our conclusion that the very extended X-ray emission of NGC 1068 is associated with the starburst disk.

By extrapolating our measured flux to higher energies, the flux of the starburst disk in the 2–10 keV band is predicted to be 2.5×10^{-12}, 5.8×10^{-12}, and 8.4×10^{-12} ergs cm^{-2} s^{-1} for a 2 keV (the minimum temperature of a spiral galaxy disk in the 0.5–3.0 keV band; Fabbiano & Trinchieri 1987) thermal spectrum, a 5 keV thermal spectrum, and an $\alpha_E = 0.5$ power-law spectrum, respectively. These numbers may be compared with the measured fluxes of $F(2\text{–}10\ \mathrm{keV}) = 6.1 \times 10^{-12}$ (Elvis & Lawrence 1988), 5.0×10^{-12} (Koyama et al. 1989), and 3.4×10^{-12} ergs cm^{-2} s^{-1} (K. A. Weaver, private communication, from a BBXRT observation). The observed spectrum of the 2–10 keV emission can be represented by a power law with $\alpha_E = 0.5 \pm 0.05$ or thermal emission with $kT > 27$ keV (Koyama et al. 1989). The emission from the starburst overpredicts the observed 2–10 keV flux for these spectral parameters. *Thus emission from the starburst may account for most or all of the hard spectrum emission seen in the* 2–10 keV *band.* An alternative interpretation, which cannot be ruled out at present, is that the apparent hard spectrum of the starburst in the *ROSAT* band results from strong Fe L line emission near 1 keV. In any case, it is likely that some part of the Fe K line emission seen from NGC 1068 (Koyama et al. 1989) originates from X-ray binaries in the starburst. A contribution from the blocked Seyfert nucleus is also probably present, for the total observed Fe K equivalent width of 2.9 keV (Marshall et al. 1992) is much larger than can be expected from an ensemble of X-ray binaries.

In constraining their models of the nuclear scattering cone, Miller, Goodrich, & Mathews (1991) required the optical depth to photoelectric absorption through this region $\tau(1\ \mathrm{keV}) \leq 1$. However, we have argued that most of the hard spectrum emission near this energy is probably from the starburst. Further, the steep spectrum, soft emission from the nucleus is partially resolved in our image, so much of this component may come from outside the electron scattering zone. Therefore, it is no longer necessary to demand that the scattering cone in NGC 1068 be optically thin to photoelectric absorption below a few keV. The removal of this observational constraint permits a greater range of model parameters for this region (see Miller, Goodrich, & Mathews, their Table 4).

4. CONCLUSIONS

The chief conclusions of this paper are as follows:

1. An X-ray map of NGC 1068 reveals an unresolved nuclear source, extended ($\simeq 1.5$ kpc) emission around the nucleus, and extended ($\simeq 13$ kpc) emission from the starburst disk. Since spatially extended, soft X-ray emission is now known in several other Seyfert galaxies (Elvis et al. 1990), their spatially integrated, soft X-ray spectra *cannot* be directly interpreted in terms of emission processes near the black hole or accretion disk, unless time variability is observed.

2. The extended circumnuclear emission aligns toward the NE, the same direction as found for the resolved emission of the active nucleus in several other wavebands.

3. While it is hard to rule out synchrotron radiation, inverse Compton scattering, and electron-scattered nuclear radiation, we prefer thermal emission from a hot wind as the source of the steep-spectrum, nuclear, and circumnuclear emission. The thermal pressure of this hot gas is similar to that of the low density component of the narrow-line region, suggesting confinement of the narrow-line clouds in the hot wind.

4. The disk of NGC 1068 has ratios of soft X-ray to B band and soft X-ray to 60 μm luminosities which are similar to those found for other starburst systems.

5. The X-ray spectrum of the starburst disk is harder than that of the nuclear emission. By adopting a plausible spectrum and extrapolating our measured flux, we find that the starburst disk may well contribute most of the hard component seen in the 2–10 keV band. This result is contrary to the current prevailing opinion that this hard component originates through electron scattering of a source in the Seyfert nucleus. Some contribution from such a source may, however, still be present.

6. In view of point 5, it is no longer clear that the nuclear electron scattering cone in NGC 1068 must be optically thin to photoelectric absorption near 1 keV. Because most of the steep spectrum, soft (0.1–3 keV) nuclear X-rays could also come from

outside the scattering cone, there is no compelling reason to believe that this region is optically thin to photoelectric absorption at *any* energy below a few keV.

We are grateful to Larry David, Gail A. Reichert, Eric M. Schlegel, T. Jane Turner, and Martin Zombeck for assistance with the data analysis, and to Pepi Fabbiano, Richard E. Griffiths, Tim M. Heckman, Julian H. Krolik, and Jean H. Swank for discussions. This research was supported by NASA grants NAG5-1532 and NAGW-2689 to the University of Maryland, and NAG5-1536 to SAO.

REFERENCES

Antonucci, R. R. J., & Miller, J. S. 1985, ApJ, 297, 621
Baldwin, J. E., Wilson, A. S., & Whittle, M. 1987, ApJ, 319, 84
Balick, B., & Heckman, T. M. 1985, AJ, 90, 197
Bruhweiler, F. C., Truong, K. Q., & Altner, B. 1991, ApJ, 379, 596
Cecil, G., Bland, J., & Tully, R. B. 1990, ApJ, 355, 70
Clements, E. D. 1981, MNRAS, 197, 829
de Vaucouleurs, G., de Vaucouleurs, A., & Corwin, H. G. 1976, Second Reference Catalogue of Bright Galaxies (Austin: University of Texas Press)
Elvis, M., Fassnacht, C., Wilson, A. S., & Briel, U. 1990, ApJ, 361, 459
Elvis, M., & Lawrence, A. 1988, ApJ, 331, 161
Evans, I. N., Ford, H. C., Kinney, A. L., Antonucci, R. R. J., Armus, L., & Caganoff, S. 1991, ApJ, 369, L27
Fabbiano, G., Feigelson, E., & Zamorani, G. 1982, ApJ, 256, 397
Fabbiano, G., & Trinchieri, G. 1985, ApJ, 296, 430
———. 1987, ApJ, 315, 46
Griffiths, R. E., & Padovani, P. 1990, ApJ, 360, 483
Koyama, K., Inoue, H., Tanaka, Y., Awaki, H., Takano, S., Ohashi, T., & Matsuoka, M. 1989, PASJ, 41, 731
Krolik, J. H., & Vrtilek, J. M. 1984, ApJ, 279, 521
Lynds, R., et al. 1991, ApJ, 369, L31
Marshall, F. E., et al. 1992, in Proc. 28th Yamada Conf., Frontiers of X-Ray Astronomy, in press
Miller, J. S., Goodrich, R. W., & Mathews, W. G. 1991, ApJ, 378, 47
Monier, R., & Halpern, J. P. 1987, ApJ, 315, L17
Pogge, R. W. 1989, ApJ, 345, 730
Raymond, J. C., & Smith, B. W. 1977, ApJS, 35, 419
Sandage, Allan. 1961, The Hubble Atlas of Galaxies (Washington, DC: Carnegie Institution of Washington)
Scoville, N. Z., Matthews, K., Carico, D. P., & Sanders, D. B. 1988, ApJ, 327, L61
Shields, G. A., & Oke, J. B. 1975, ApJ, 197, 5
Telesco, C. M., Becklin, E. E., Wynn-Williams, C. G., & Harper, D. A. 1984, ApJ, 282, 427
Tresch-Fienberg, R., Fazio, G. G., Gezari, D. Y., Hoffmann, W. F., Lamb, G. M., Shu, P. K., & McCreight, C. R. 1987, ApJ, 312, 542
Ulvestad, J. S., Neff, S. G., & Wilson, A. S. 1987, AJ, 93, 22
Wilson, A. S., & Ulvestad, J. S. 1982, ApJ, 263, 576
———. 1987, ApJ, 319, 105